Cancer Cell
Article

Dependency of Colorectal Cancer on a TGF-β-Driven Program in Stromal Cells for Metastasis Initiation

Alexandre Calon,[1,11] Elisa Espinet,[1,11] Sergio Palomo-Ponce,[1] Daniele V.F. Tauriello,[1] Mar Iglesias,[4] María Virtudes Céspedes,[5] Marta Sevillano,[1] Cristina Nadal,[6] Peter Jung,[1] Xiang H.-F. Zhang,[7] Daniel Byrom,[2] Antoni Riera,[2,8] David Rossell,[3] Ramón Mangues,[5] Joan Massagué,[7,9] Elena Sancho,[1,*] and Eduard Batlle[1,10,*]
[1]Oncology Programme
[2]Chemistry and Molecular Pharmacology Programme
[3]Biostatistics and Bioinformatics Unit
Institute for Research in Biomedicine, 08028 Barcelona, Spain
[4]Pathology Department, Hospital del Mar, Institut Hospital del Mar d'Investigacions Mèdiques and Autonomous University of Barcelona, 08004 Barcelona, Spain
[5]Biomedical Research Institute Sant Pau, Hospital de la Santa Creu i Sant Pau and CIBER de Bioingeniería, Biomateriales y Nanomedicina, 08025 Barcelona, Spain
[6]Institut de Malalties Hemato-Oncològiques, Hospital Clínic-CIBERehd, 08036 Barcelona, Spain
[7]Cancer Biology and Genetics Program, Memorial Sloan-Kettering Cancer Center, New York, NY 10021, USA
[8]Departament de Quimica Organica, Universitat de Barcelona, 08028 Barcelona, Spain
[9]Howard Hughes Medical Institute, Chevy Chase, MD 20185, USA
[10]Institució Catalana de Recerca i Estudis Avançats (ICREA), 08010 Barcelona, Spain
[11]These authors contributed equally to this work
*Correspondence: elena.sancho@irbbarcelona.org (E.S.), eduard.batlle@irbbarcelona.org (E.B.)
http://dx.doi.org/10.1016/j.ccr.2012.08.013

SUMMARY

A large proportion of colorectal cancers (CRCs) display mutational inactivation of the TGF-β pathway, yet, paradoxically, they are characterized by elevated TGF-β production. Here, we unveil a prometastatic program induced by TGF-β in the microenvironment that associates with a high risk of CRC relapse upon treatment. The activity of TGF-β on stromal cells increases the efficiency of organ colonization by CRC cells, whereas mice treated with a pharmacological inhibitor of TGFBR1 are resilient to metastasis formation. Secretion of IL11 by TGF-β-stimulated cancer-associated fibroblasts (CAFs) triggers GP130/STAT3 signaling in tumor cells. This crosstalk confers a survival advantage to metastatic cells. The dependency on the TGF-β stromal program for metastasis initiation could be exploited to improve the diagnosis and treatment of CRC.

INTRODUCTION

Most colorectal cancers (CRCs) originate from the intestinal epithelium as premalignant lesions called adenomas. Over time, a small fraction of adenomas are transformed to CRCs because of the accumulation of genetic alterations in a small set of driver genes, including *KRAS*, *TP53*, *SMAD4*, or *PIK3CA* (Markowitz and Bertagnolli, 2009). Alterations in these and other cancer-causing genes have been associated with the different stages of the progression of the tumor (i.e., transition from normal intestinal mucosa to adenoma and further progression to CRC). In contrast, metastases that are either present at the time of diagnosis or develop as distant relapses after therapy are not strongly associated with alterations in any of these key

Significance

About 40%–50% of all patients with colorectal cancer will present with metastasis either at the time of diagnosis or as recurrent disease upon intended curative therapy. In the absence of genetic alterations that explicate these processes, it remains a major challenge to predict which patients will develop metastatic disease or to design targeted therapies. Here, we show that metastasis depends on a gene program expressed by the tumor microenvironment upon TGF-β stimulation. Low stromal TGF-β signaling is a robust predictor of disease-free survival after therapy, which improves on the current AJCC staging system. Furthermore, colonization of foreign organs requires TGF-β signaling in stromal cells and therefore may be a target for therapeutic intervention at early time points of the metastatic process.

genes (Walther et al., 2009). In addition, global genome sequencing of metastatic lesions and primary CRCs revealed hardly any metastasis-specific mutation (Jones et al., 2008). This drawback has hampered the development of metastasis-specific therapies, as well as the identification of patients with CRC at risk of suffering metastatic disease.

Mutational inactivation of the TGF-β signaling pathway is key during CRC progression. Alterations in TGF-β pathway components are first detected in advanced adenomas and affect 40%–50% of all CRCs (Markowitz et al., 1995; Markowitz and Bertagnolli, 2009). In mouse models, mutations in the tumor suppressor *Apc* combined with inactivation of TGF-β signaling components in epithelial intestinal cells trigger the development of invasive adenocarcinomas (Muñoz et al., 2006; Takaku et al., 1998). Restoration of a functional TGF-β pathway in human CRC cells abrogates proliferation and tumorigenicity (Wang et al., 1995), implying that TGF-β signaling exerts tumor-suppressive effects. Hence, it has been proposed that TGF-β imposes a selective pressure during CRC progression, which tumors avert by genetic inactivation of the TGF-β receptors (*TGFBR1* and *TGFBR2*) or of the SMAD intracellular mediators (*SMAD4*, *SMAD2*, and *SMAD3*) (Grady and Markowitz, 2002; Markowitz et al., 1995; Markowitz and Bertagnolli, 2009).

In addition to its tumor suppressor role in epithelial cells, TGF-β signaling also acts as a negative regulator of tumor formation by conditioning mucosa-resident stromal cells. Mice with a deletion of *Smad4* in T cells develop gastrointestinal tumors (Hahn et al., 2011; Kim et al., 2006). Similarly, transgenic expression of a dominant negative TGFBR2 in T cells accelerates azoxymethane-induced colon carcinogenesis (Becker et al., 2004). In both cases, T cells lacking TGF-β signals exacerbate the production of proinflammatory cytokines that spark off the transformation of the colonic epithelium (Becker et al., 2004; Kim et al., 2006).

Although the above genetic and mutational data support a tumor suppressor role for TGF-β signaling in intestinal carcinogenesis, high levels of TGFB1 in the serum of patients with CRC are associated with poor outcome in the clinical setting (Tsushima et al., 2001). The relevance of TGF-β signaling for disease progression has been widely recognized in tumors where cancer cells retain a functional TGF-β pathway, such as breast or prostate cancer (Massagué, 2008). In these tumor cells, TGF-β induces a variety of prometastatic programs that range from induction of epithelial-to-mesenchymal transition to expression of genes that allow colonization of foreign organs (Massagué, 2008). It is less clear, however, what CRC cells can gain from high TGF-β levels once the pathway is fully inactivated by mutations and how this phenomenon links to an adverse outcome. To address this apparent paradox, we investigated whether TGF-β may activate the tumor microenvironment to assist CRC cells in the metastatic process.

RESULTS

TGF-β Levels in CRC Are a Robust Predictor of Disease Relapse

We first investigated whether differences in TGF-β levels in primary tumors were associated with clinical disease progression in CRC. To this end, we interrogated a representative pooled cohort of 345 cases treated at three different hospitals for which transcriptomic profiles and clinical follow-up were publicly available. In this metacohort, overall TGF-β levels were low in patients with American Joint Cancer Committee (AJCC) stage I cancer, compared to cancer at more advanced stages (Figure 1A; see Tables S1 and S2 available online). The AJCC staging system has limited power to predict disease relapse, because 10%–20% of patients with stage II CRC and 30%–50% of patients with stage III CRC will develop recurrent cancer after therapeutic intervention. We found that, for every increase in overall TGF-β (*TGFB*) expression, the risk of cancer recurrence augmented by 83% (Figure 1B). As a consequence, we observed large differences in the frequency of disease relapse after therapy in patients bearing tumors with high, medium, or low *TGFB* (Figure 1C) or individual TGF-β isoform levels (Figures S1A and S1B). During 10 years of follow-up, only patients with medium or high *TGFB* expression in the primary tumor (53 of 220 patients) suffered cancer recurrence. Remarkably, all patients bearing *TGFB*-low tumors remained disease-free (Figure 1C, blue group). High *TGFB* levels were robustly associated with relapse in patients with stage II and III cancer, whereas low *TGFB* characterized a small set of patients with no observed recurrences in both stages (Figure 1D; 17% and 11% of patients with cancer at these stages, respectively). The rare relapses occurring in stage I CRCs (2 of 35 patients in this group) also expressed high *TGFB* levels (Figure 1D), although this comparison did not reach statistical significance, probably because of the low incidence of recurrences in this stage. Cox proportional hazards multivariate analysis demonstrated that *TGFB* expression is an independent predictor of cancer recurrence that outperforms AJCC staging system in the identification of patients with CRC who remained disease free upon therapy (Figure 1E). The predictive power of *TGFB* levels also compared favorably to that of other genes that have been repeatedly associated with disease relapse in CRC (Table S3).

TGF-β Response Signatures in Tumor-Associated Stromal Cells Predict Disease Relapse in CRC

An increase in TGF-β isoform levels was evident at the adenoma-CRC transition, as shown by expression profiling of a small cohort of colon tumors (Figure S1C). Nuclear p-SMAD3, a marker for TGF-β signaling, stained predominantly the stromal compartment in most CRCs (Figure S1D). In the majority of samples, epithelial CRC cells were markedly less stained compared to adjacent stromal cells or to the epithelial compartment of adenomas (Figures S1D–S1F). We characterized the stromal cell types stained by p-SMAD3 in CRCs but could not discriminate any obvious cell-type specificity. Rather, p-SMAD3 indiscriminately labeled all major types of stromal cells in CRCs, including T cells, macrophages, endothelial cells, and fibroblasts (Figures S2A–S2H). We thus quantified the association of TGF-β-activated stromal cell populations with disease progression. To this end, we used as surrogates the gene expression programs induced by the addition of TGF-β (TGF-β response signatures or TBRS) in cultures of normal-tissue-derived T cells (T-), macrophages (Ma-), endothelial cells (End-), or fibroblasts (F-). To avoid biases, we used the full set of genes upregulated by TGF-β signaling in these cell cultures (>2 fold, $p < 0.05$) without additional filtering or refinement (Table S4). By Gene

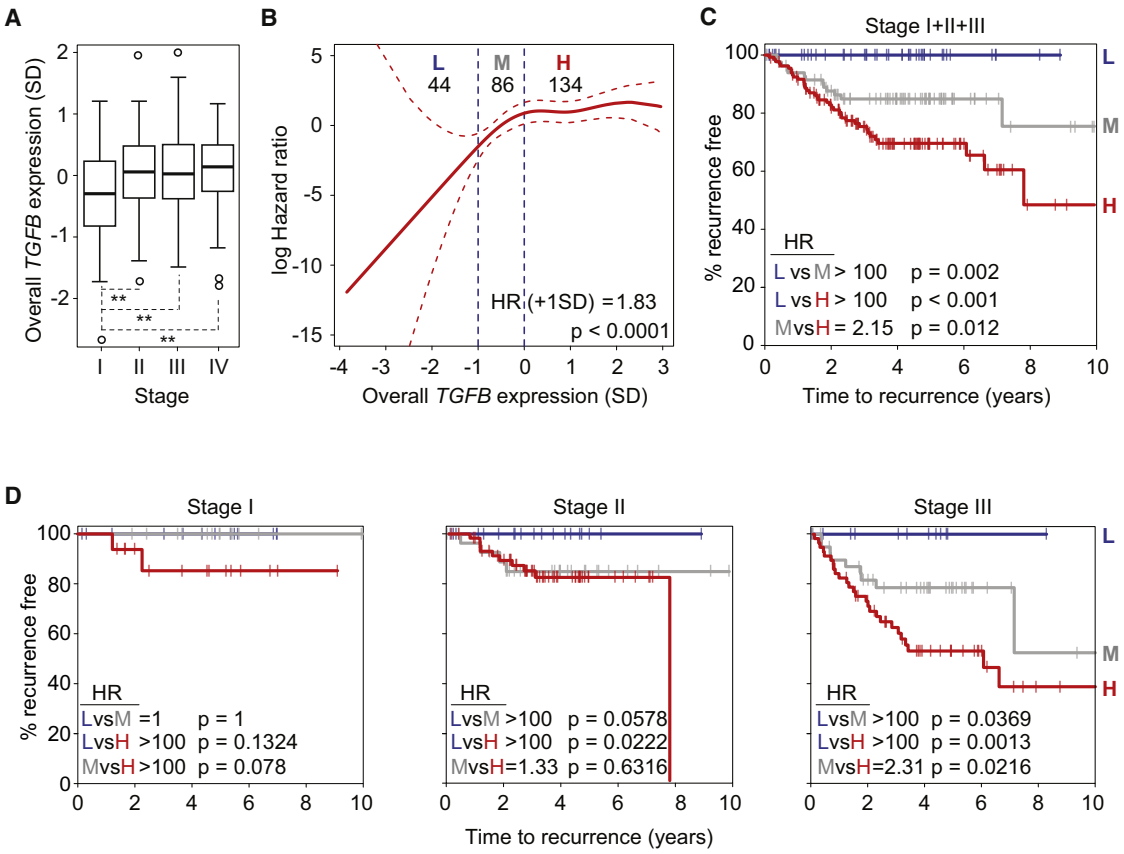

E

Overall *TGFB*	HR	CI. low	CI. up	p value
+1SD increase	1.68	1.28	2.21	0.0002
High *vs* Low	>100	NA	NA	<0.0001
Medium *vs* Low	>100	NA	NA	0.0043
High *vs* Medium	2.00	1.07	3.76	0.0231
AJCC stage	NA	NA	NA	0.0002
Stage II *vs* I	2.56	-1.74	11.40	0.1685
Stage III *vs* I	6.84	1.62	28.84	0.0006
Stage III *vs* II	2.67	1.43	4.98	0.0011
study	NA	NA	NA	0.0011

Figure 1. High TGF-β Expression Predicts CRC Relapse

(A) Overall *TGFB* mRNA expression in CRC stages I–IV. Values are z-scores with standard deviation (SD) from the mean (**p < 0.01, two-tailed Student's t test).

(B) Smooth function correlates overall *TGFB* mRNA expression with relative risk of recurrence. Patients with stage IV cancer were excluded from this analysis. Red dashed lines: 95% confidence interval (CI). Blue dashed lines: thresholds for patient selection into groups with low (L; blue, 44 patients), medium (M; gray, 86 patients), and high (H; red, 134 patients) *TGFB* expression; p values and increase in HR per each increase in standard deviation of expression (+1 SD) are shown.

(C and D) Kaplan-Meier plots display recurrence-free survival (RFS) over time (C) and grouped by AJCC stage (D) for groups defined in (B) . HR and p values compare RFS over time for patients grouped according to *TGFB* levels (L versus M, L versus H, and M versus H).

(E) Cox proportional hazards multivariate analysis of TGF-β expression and AJCC staging in identifying patients who remained disease-free upon therapy.

See also Figure S1.

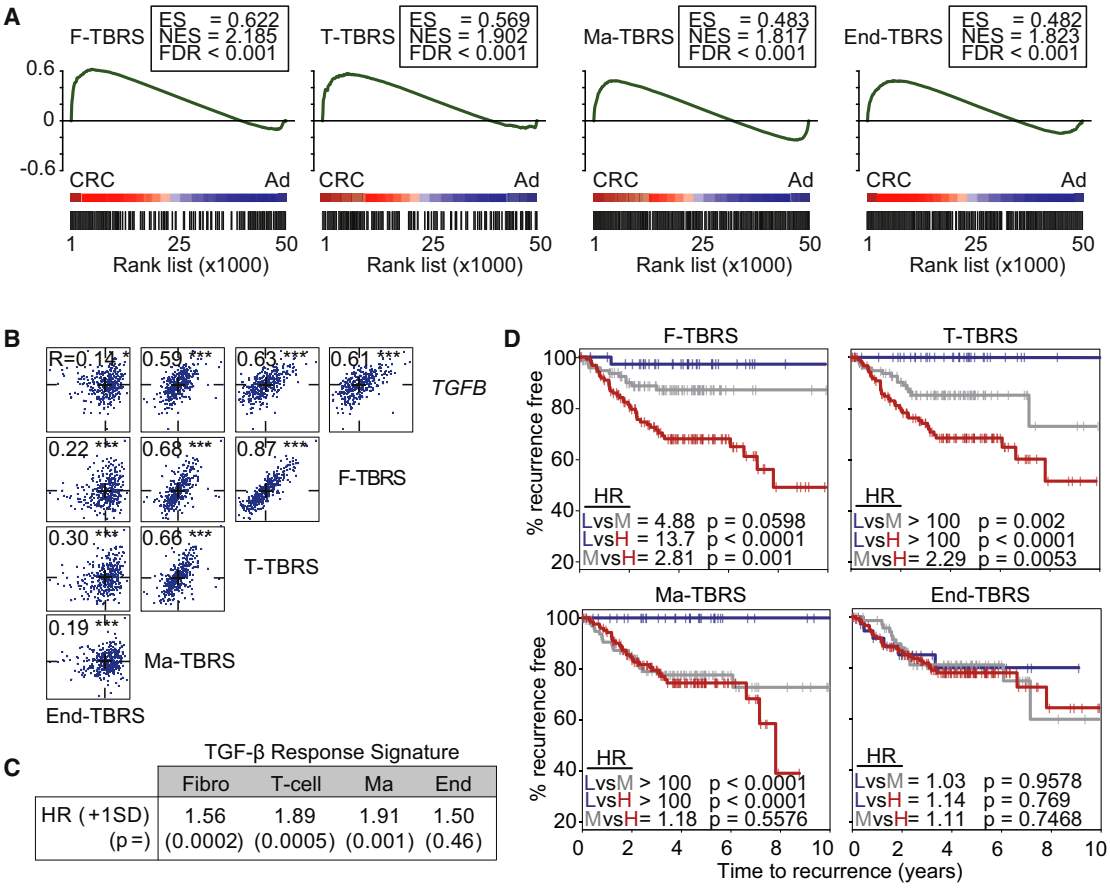
A
F-TBRS
ES = 0.622
NES = 2.185
FDR < 0.001
T-TBRS
ES = 0.569
NES = 1.902
FDR < 0.001
Ma-TBRS
ES = 0.483
NES = 1.817
FDR < 0.001
End-TBRS
ES = 0.482
NES = 1.823
FDR < 0.001
CRC
Ad
Rank list (x1000)
B
TGFB
F-TBRS
T-TBRS
Ma-TBRS
End-TBRS
C
TGF-β Response Signature
Fibro
T-cell
Ma
End
HR (+1SD)
(p=)
1.56
(0.0002)
1.89
(0.0005)
1.91
(0.001)
1.50
(0.46)
D
% recurrence free
HR
LvsM = 4.88 p = 0.0598
LvsH = 13.7 p < 0.0001
MvsH= 2.81 p = 0.001
LvsM > 100 p = 0.002
LvsH > 100 p < 0.0001
MvsH= 2.29 p = 0.0053
LvsM > 100 p < 0.0001
LvsH > 100 p < 0.0001
MvsH= 1.18 p = 0.5576
LvsM = 1.03 p = 0.9578
LvsH = 1.14 p = 0.769
MvsH= 1.11 p = 0.7468
Time to recurrence (years)
E
Primary CRCs
Cell sorting
Epithelial cells
EPCAM+ CD45- CD31- FAP-
Leukocytes
EPCAM- CD45+ CD31- FAP-
Endothelial cells
EPCAM- CD45- CD31+ FAP-
CAFs
EPCAM- CD45- CD31- FAP+
F
KRT20
EPCAM
CDH1
DCN
α-SMA
PDPN
CD45
CD2
CD19
VWF
CDH5
ICAM2
Leukocytes
Epithelial
Endothelial
CAFs
G
All genes
Relative expression vs. Epithelial (log2)
T-TBRS
Ma-TBRS
End-TBRS
F-TBRS
H
Genes predicting recurrence (HR > 1, p < 0.05)

Set Enrichment Analysis (GSEA) (Subramanian et al., 2005), we determined that all stromal TBRSs were highly enriched in CRCs compared to adenomas (Figure 2A). Importantly, the expression levels of *TGFB*, F-TBRS, T-TBRS, and Ma-TBRS showed robust direct correlations in the cohort of patients with CRC (Figure 2B), implying that they are, to a large extent, concurrently expressed in CRC. Significantly, these three signatures were excellent predictors of disease relapse in patients with stage I, II, and III CRC and segregated a low-expression patient group with virtually no risk of developing recurrent cancer after therapy (Figures 2C and 2D, blue group). This result paralleled that obtained with *TGFB* levels (Figure 1). In patients with stage IV CRC who underwent potential curative therapy, high *TGFB* and stromal TBRS expression levels also correlated with higher risk of relapse (Figures S2I–S2L). However, a large proportion of these patients with stage IV disease eventually experienced relapse, likely because of the lack of effective therapies to eliminate an overt metastatic disease. Consistent with their ability to predict disease progression, the stromal TBRS included several well-known prometastatic genes, such as *ANGPTL4* (Padua et al., 2008), *PTHLH* (Yin et al., 1999), *HBEGF* (Bos et al., 2009), *CTGF* (Kang et al., 2003), *TNC* (Oskarsson et al., 2011), or *JAG1* (Sethi et al., 2011; Sonoshita et al., 2011), all of which encode for secreted or membrane-bound factors (Table S4).

To further analyze the cell-type-specific expression of each stromal TBRS in vivo, we purified by FACS various cell populations from fresh CRC samples and assessed their gene expression profiles (Figures 2E and 2F). Relative levels of cell-type-specific marker genes confirmed the purification of epithelial tumor cells (EPCAM$^+$), leukocytes (CD45$^+$), endothelial cells (CD31$^+$), and fibroblasts (FAP$^+$) (Figure 2F). A global comparative analysis revealed a trend toward high levels of all stromal TBRS in FAP$^+$ CAFs. Conversely, epithelial tumor cells expressed the lowest levels of each stromal TBRS (Figure 2G). Remarkably, these trends became very significant for those genes within the T-TBRS, Ma-TBRS, or End-TBRS that associated positively with cancer relapse (HR > 1, $p < 0.05$; Figure 2H). Although the in vitro derived End-TBRS did not predict disease progression (Figures 2C and 2D), we observed elevated expression of recurrence-associated TGF-β target genes in endothelial cells directly purified from tumors (Figure 2H). This observation may suggest that the response of in vitro cultured endothelial cells to TGF-β signaling deviates significantly from that occurring in the tumor microenvironment. Altogether, these data highlight that the response of stromal cells to TGF-β is an accurate predictor of disease relapse in patients with CRC. Although high *TGFB* levels activate gene programs in a wide range of tumor-associated stromal cell types, our in vivo data indicate that CAFs and, to a lesser extent, endothelial cells are the main contributors to the association of stromal TGF-β-driven programs with poor outcome after therapy.

TGF-β Signaling in the Stroma Promotes Tumor Initiation

The above data suggest the possibility that elevated *TGFB* levels in CRC influence disease progression by acting on stromal cells. To functionally dissect this effect without the interference of TGF-β signaling in epithelial cancer cells, we took advantage of the fact that virtually all late-stage CRC-derived cell lines display mutational inactivation of the TGF-β pathway. These CRC cell lines, however, did not induce robust stromal TGF-β responses when injected into nude mice, as shown by the lack of p-SMAD2 accumulation in tumor-associated stromal cells (arrows in Figures 3A and 3B; data not shown). To enforce high TGF-β signaling in xenografts, we engineered CRC cell lines to secrete active TGFB1. Subcutaneous tumors obtained from HT29-M6$^{TGF\text{-}\beta}$, KM12L4a$^{TGF\text{-}\beta}$ and SW48$^{TGF\text{-}\beta}$ cells contained abundant p-SMAD2$^+$ stromal cells (arrowheads in Figures 3A and 3B; data not shown) and increased expression levels of stromal TBRS genes (Figure 3C; data not shown). Importantly, secretion of TGF-β did not induce autocrine responses in these CRC cells (i.e., SMAD reporter activity, proliferation, or EMT induction; Figures S3A–S3D), owing to homozygous mutations in *TGFBR2* in KM12L4a and in SW48. HT29-M6 cells carry homozygous inactivation of the *SMAD4* locus, which rendered this cell line unresponsive to TGF-β (Figures S3A–S3D). Yet, this genetic alteration did not impede the nuclear accumulation of p-SMADs (Figure 3B), as previously reported for other *SMAD4* mutant cell lines (Alarcón et al., 2009; Liu et al., 1997). Therefore, the xenografts derived from these cells combine a TGF-β response in tumor stromal cells with lack of TGF-β signaling in cancer cells, the scenario characteristic of advanced CRC. We inoculated CRC cells subcutaneously into nude mice in quantities that generated suboptimal engraftment in control conditions (see Experimental Procedures). Elevated levels of

Figure 2. Stromal TGF-β Gene Signatures Predict Recurrence

(A) Gene set enrichment analyses (GSEA) of TGF-β response signatures (TBRS) of Fibroblasts (F-TBRS), T cells (T-TBRS), macrophages (Ma-TBRS), or endothelial cells (End-TBRS) in carcinoma versus adenoma samples. ES, enrichment score; NES, normalized enrichment score; FDR, false discovery rate.

(B) Cross-correlations between *TGFB*, F-TBRS, T-TBRS, Ma-TBRS, and End-TBRS in the patient cohort. Blue dots, patients. R, correlation coefficients. Values are Z scores (*$p < 0.05$, ***$p < 0.001$).

(C) The p values and increase in HR per each increase in expression (+1SD) in F-TBRS, T-TBRS, Ma-TBRS, and End-TBRS were obtained via Cox proportional Hazards model.

(D) Kaplan-Meier plots display RFS of patients with low (blue), medium (gray), or high (red) F-TBRS, T-TBRS, Ma-TBRS, or End-TBRS expression levels.

(E) FACS-purification of cell populations from primary CRC samples, enriched in the indicated cell types.

(F) Heat map shows relative expression levels of marker genes for epithelial (blue), leukocyte (red), endothelial (orange) cells, and cancer-associated fibroblasts (green) in each cell population. Values are normalized intensities, log2.

(G) Relative expression of each TBRS in cell populations from (F). Whiskers represent minimum (Vmin) and maximum (Vmax) values, truncated at 1.5 times the interquartile range (log2; *$p < 0.05$, **$p < 0.01$, Student's t test).

(H) Relative expression in each cell population of genes within the T-TBRS, Ma-TBRS, End-TBRS, or F-TBRS associating positively with relapse. Whiskers: Vmin, Vmax (log2; *$p < 0.05$, **$p < 0.01$, Student's t test).

See also Figure S2.

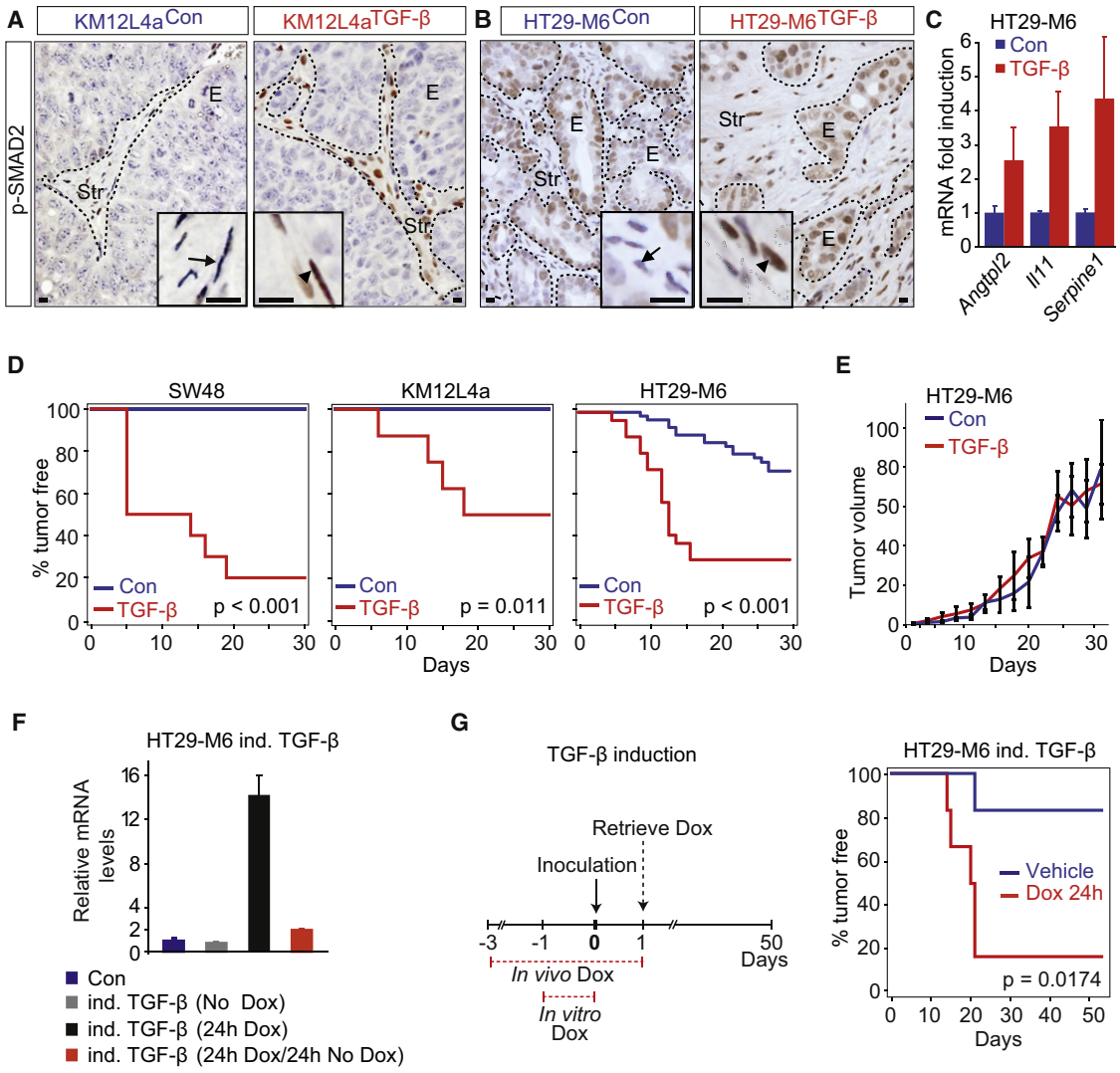

Figure 3. TGF-β Activated Stroma Induces Tumor Initiation

(A and B) Nuclear p-SMAD2 reactivity (arrowheads) in subcutaneous (s.c.) tumors derived from TGF-β-secreting KM12L4a (A) or HT-29M6 (B) CRC cells and control cells. E, epithelial cells; Str, stromal cells. Scale bars = 10 μm.

(C) Relative expression of some stromal TBRS genes in tumors from (B). Values are mean ± SEM (n = 3).

(D) Kaplan-Meier plots display tumor-free survival (TFS) for mice injected s.c. with 3×10^4 TGF-β-secreting (red) or control cell lines (blue); SW48 (n = 8); KM12L4a (n = 8); HT29-M6 cells (n = 25 (red), n = 39 (blue).

(E) Growth over time for HT29-M6$^{TGF-\beta}$ (red; n = 13) and HT29-M6^{Con} (blue; n = 16) derived tumors. Day 1: day of first detection. Values are mean ± SEM.

(F) Relative *TGFB* mRNA levels in HT29-M6 cells expressing active TGF-β through a doxycycline (Dox)-inducible promoter (HT29-M6 ind. TGF-β) compared to control cells (Con, blue). Inducible TGF-β cells were nontreated (gray), treated with Dox for 24 hr (black), or treated with Dox for 24 hr followed by 24 hr of Dox withdrawal prior to qRT-PCR (red). Values are mean ± SD (n = 3).

(G) Inducible TGF-β cells were either untreated (blue) or pretreated with Dox in vitro 24 hr before s.c. inoculation (3×10^4 cells; n = 6). Recipient mice received either Dox (red) or vehicle (blue) in drinking water ad libitum during 3 days prior to injection. Kaplan-Meier curves show TFS when TGF-β secretion is induced in vivo for 24 hr (red) compared to control cells (blue).

See also Figure S3.

TGF-β dramatically increased the frequency of tumor formation and reduced the latency period in all cell lines (Figure 3D). Yet, after tumor initiation, the TGF-β-activated microenvironment had no effect on xenograft growth rates (Figure 3E; data not shown). We further tested this early requirement by controlling the timing of TGF-β production in HT29-M6 CRC cells via a doxycycline-inducible promoter (Figures 3F and 3G). Secretion of TGF-β during the first 24 hr following inoculation of tumor cells was sufficient to enhance tumor initiation (Figure 3G). Given the well-established role of TGF-β in the polarization and suppression of the immune system in tumors (Flavell et al., 2010), we tested whether the enhancement of tumor initiation by TGF-β signaling could be explained by modulation of the immune system. To this end, we injected CRC cells in severely

immunocompromised mice of the NOD/SCID interleukin-2 receptor gamma chain null strain (NSG) (Shultz et al., 2007). In these NSG mice, high TGF-β levels were also capable of enhancing tumor initiation, although fewer cancer cells were required to form tumors in this strain (Figure S3E).

Stromal TGF-β Signaling Is Required for Efficient Metastasis Initiation

CRCs at stages I, II, and III displaying low stromal TGF-β signaling fail to form recurrences, which, in most patients with CRC, occur in the form of metastasis. To study whether stromal TGF-β signaling may influence metastasis formation, we inoculated KM12L4a^{Con} and KM12L4a$^{TGF\text{-}\beta}$ cells in the cecum of nude mice. Both cell lines gave rise to aggressive colorectal tumors, which killed mice by obstruction of the intestinal lumen. At death, KM12L4a^{Con} and KM12L4a$^{TGF\text{-}\beta}$ had generated colon tumors of equivalent size (data not shown) with no significant differences in their degree of invasion, spread to local lymph nodes, or major histological features (Figure 4A; Figures S4A and S4B). Yet, two thirds of mice bearing KM12L4a^{Con} colon tumors remained metastasis free, whereas 10 of 11 mice inoculated with KM12L4a$^{TGF\text{-}\beta}$ cells developed lung and/or liver metastasis ($p < 0.01$, Figure 4B). These data imply that stromal TGF-β signaling promotes metastasis formation. We further explored this phenomenon by using intrasplenic inoculation of CRC cells (Morikawa et al., 1988). Secretion of TGF-β by KM12L4a cells increased the liver metastases burden in mice (Figure 4C). We also observed a large increase in the number of liver metastases generated by HT29-M6 secreting TGF-β (Figure 4D). In addition, a significant fraction of mice inoculated with KM12L4a$^{TGF\text{-}\beta}$ or HT29-M6$^{TGF\text{-}\beta}$ developed lung metastases, implying that TGF-β signaling also facilitated secondary organ colonization (Figure 4E). The kinetics of liver metastasis revealed that control or TGF-β secreting cells expanded with similar rates once tumor cells had taken root and resumed growth (from day 7 in Figure 4F). However, during the first few days following inoculation, most KM12L4a^{Con} cells that reached the liver were progressively lost, and by 7 days, tumor cells were barely detectable (Figure 4F). A virtually complete loss of control metastatic cells was noticed during the first 24 hr upon inoculation of lower tumor cell numbers (Figure S4C). Secretion of TGF-β significantly increased the amounts of KM12L4a cells detected at these early time points (Figure 4F; Figure S4C). To further test this early requirement, we used CRC cells that expressed TGF-β from a doxycycline-inducible promoter. A short pulse of TGF-β (24 hr) at the moment of intrasplenic inoculation was sufficient to increase metastasis burden by facilitating metastasis initiation without affecting subsequent tumor growth (Figures 4G and 4H; Figure S4D; $p < 0.05$). Thus, high levels of TGF-β specifically act to enhance the colonization capability of CRC cells at the initial phase of metastasis. Because KM12L4a and HT29-M6 cells harbor an inactivated TGF-β pathway, enhanced metastasis initiation by TGF-β secretion must be the consequence of changes in the tumor microenvironment. Indeed, metastasis derived by both TGF-β secreting cell lines displayed enhanced desmoplastic reaction (Figures S4E–S4L) with abundant p-SMAD2 accumulation in stromal cells (Figures 4I and 4J; Figures S4M and S4N) and elevated expression of stromal TBRS genes (Figure 4K; data not shown).

Pharmacological Inhibition of Stromal TGF-β Signaling Blocks Metastasis Initiation

We have recently described the purification of Colon Cancer Stem Cells (CoCSCs) from CRC biopsies via surface expression of the receptor tyrosine kinase EPHB2 (Merlos-Suárez et al., 2011). We isolated EPHB2-high CoCSCs from the primary tumor of a patient with stage IV CRC and cultured them in conditions similar to those used for expansion of normal colon stem cells (Jung et al., 2011; Sato et al., 2011). EPHB2-high tumor cells embedded in matrigel expanded as epithelial tumor organoids (Figure 5A), which retained high expression levels of colon stem cell marker genes such as *LGR5* and *ASCL2* (data not shown). Genomic analysis of the tumor organoids revealed that the two *TGFBR2* alleles were inactivated by mutations in this patient (data not shown). Indeed, treatment with TGFBR1-specific inhibitor LY2157299 (Bueno et al., 2008) or the addition of active TGF-β did not modify in vitro growth rates, morphology, or organoid forming activity of this CoCSC-derived culture (Figures 5A–5C). Primary CoCSCs expressed higher *TGFB* levels than did CRC cells lines (Figure 5D). When injected in immunodeficient mice, they generated tumors with abundant p-SMAD2^{+} stromal cells (Figure 5E, left panel), implying that this primary CoCSCs elicited a TGF-β response in the tumor microenvironment. Feeding mice bearing macroscopic tumors from CoCSCs-derived cultures with LY2157299 blocked TGF-β signaling in the tumor stroma as shown by reduced stromal p-SMAD2 positivity (Figure 5E, right panel) and downregulated levels of stromal TBRS genes (Figure 5F). Importantly, treatment with LY2157299 conferred resistance to the formation of subcutaneous tumors by primary CoCSC-derived cells (Figures 5G and 5H). Remarkably, this TGF-β inhibitor regime also reduced formation of liver metastasis by CoCSCs inoculated via the spleen (Figures 5I and 5J). Kinetics of metastatic colonization showed that LY2157299 reduced the number of cells that engrafted the liver immediately after inoculation (Figure 5I, inset), the opposite behavior of that induced by secretion of high TGF-β levels in CRC cell lines. Of note, these experiments were performed in NSG mice, which rules out that LY2157299 blocked metastasis through changes in the function of the immune system. Altogether, the clinical and functional data described so far indicate that a TGF-β program activated in the tumor microenvironment confers CRC cell competence to overcome the initial phase of metastasis.

Metastasis Initiation by TGF-β-Stimulated Stromal Cells Depends on GP130/STAT3 Signaling in Tumor Epithelial Cells

We next sought to understand the mechanisms behind the potent effect of stromal TGF-β program on the capacity of CRC cells to initiate metastasis. We discovered that subcutaneous tumors and metastases generated in the context of a TGF-β activated microenvironment displayed prominent accumulation of p-STAT3 in CRC cells compared with those derived from control cells (Figure 6A; Figures S5A–S5H). STAT3 signaling depended on GP130 as shown by strong reduction of epithelial p-STAT3 levels upon GP130 shRNA-mediated knockdown in CRC cells (Figure 6A; Figures S5I and S5J). These results suggest that TGF-β induces the expression of GP130-binding cytokines in the tumor microenvironment, which in turn

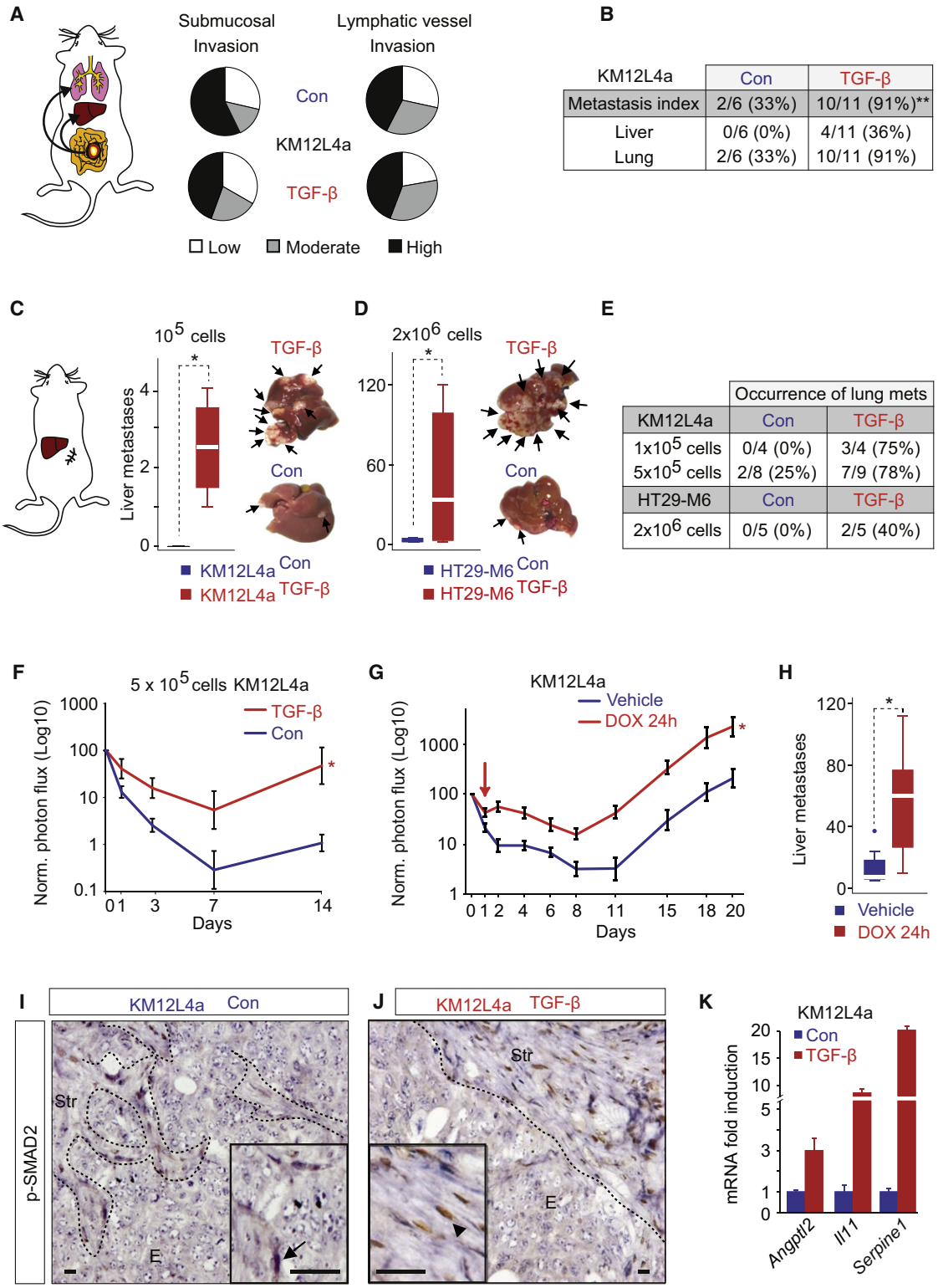

KM12L4a	Con	TGF-β
Metastasis index	2/6 (33%)	10/11 (91%)**
Liver	0/6 (0%)	4/11 (36%)
Lung	2/6 (33%)	10/11 (91%)

	Occurrence of lung mets	
KM12L4a	Con	TGF-β
$1x10^5$ cells	0/4 (0%)	3/4 (75%)
$5x10^5$ cells	2/8 (25%)	7/9 (78%)
HT29-M6	Con	TGF-β
$2x10^6$ cells	0/5 (0%)	2/5 (40%)

Figure 4. TGF-β Activated Stroma Induces CRC Metastasis

(A) Pie charts for submucosal or lymphatic vessel invasion in KM12L4a^{con}- and KM12L4a$^{TGF-β}$-derived cecum tumors.

(B) Incidence of metastases in mice from (A) (**$p < 0.01$; Fisher's exact test).

(C and D) Number of liver metastases after intrasplenic (IS) injection with 10^5 KM12L4a^{Con} or KM12L4a$^{TGF-β}$ cells (C) or 2×10^6 HT29-M6^{Con} or HT29-M6^{TGF-b} cells (D) (*$p < 0.05$, two-tailed Student's t test). Whiskers: Vmin, Vmax. Representative livers are shown from injections with 5×10^5 cells (C) or 2×10^6 cells (D). Arrows denote metastatic nodules.

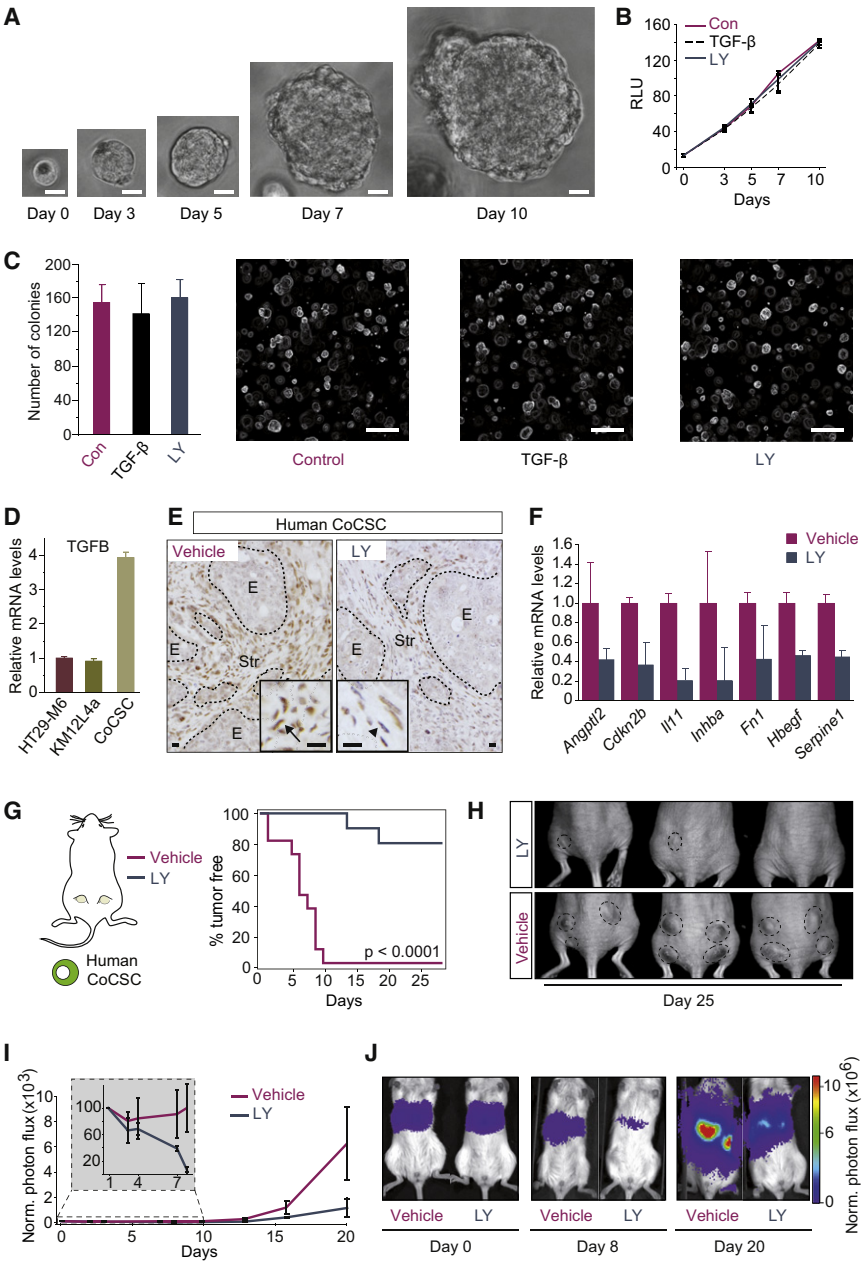

Figure 5. Inhibition of TGF-β Response in the Stroma Blocks Tumor Initiation

(A) In vitro expansion of a CoCSC. Scale bars = 10 μm.

(B) In vitro growth of human CoCSCs upon addition of TGF-β or LY2157299 (LY). Values are mean relative absorbance (RLU) over time ± SD (n = 3).

(C) Number of organoids from human CoCSCs treated with TGF-β or LY2157299. Values are mean ± SD (n = 3). Representative images are shown. Scale bars = 200 μm.

(D) qRT-PCR for *TGFB* in the indicated CRC cells. Values are mean ± SEM.

(E) p-SMAD2 staining in s.c. tumors derived from CoCSCs injected in NSG mice treated with LY2157299 for 3 days (LY; right panel, arrowhead) or untreated (left panel; arrow). E, epithelial cells; Str, stromal cells. Scale bars = 10 μm.

(F) Relative expression of some stromal TBRS genes in tumors from (E). Values are mean ± SEM (n = 2).

(G) Kaplan–Meier curves show TFS for mice injected s.c. with 10^6 CoCSCs. Mice received LY2157299 (blue) or vehicle (purple) from 3 days prior to inoculation until sacrifice (n = 12).

(H) Representative images from (G).

(I) Bioluminescence over time after IS inoculation of 5 × 10^5 CoCSCs cells in NSG mice treated as in (G). Values, normalized as in Figure 4F, are mean ± SEM.

(J) Representative images from (I).

switches on STAT3 signaling in tumor epithelial cells. To study the relevance of this signaling cycle for tumorigenesis, we inoculated subcutaneously into nude mice HT29-M6 cells that secreted active TGFB1 and at the same time were knockdown for GP130 (HT29-M6$^{shGP130/TGF-β}$). These experiments revealed that GP130/STAT3 signaling in cancer cells participated in the enhancement of tumor initiation mediated by stromal TGF-β signaling (Figure 6B), but it was not important for the growth of tumors once established (Figure 6C). HT29-M6^{shCon} or HT29-M6^{shGP130} cells grew with identical kinetics in vitro (Figure S5K) and, in the absence of a source of TGF-β, formed tumors in immunodeficient mice with equivalent latency and frequency (Figure S5L).

Importantly, these GP130-knockdown HT29-M6 cells secreting TGF-β displayed decreased liver take rates during the first hours following intrasplenic inoculation (Figures 6D and 6E) compared to control cells. After the initial phase, the number of tumor cells detected in the liver progressively decreased and, after two weeks, both HT29-M6$^{shCon/TGF-β}$ and HT29-M6$^{shGP130/TGF-β}$ cells reinitiated expansion with similar kinetics

(E) Incidence of metastasis induced in (C), (D), and (F).

(F) Normalized bioluminescence over time after injection of 5 × 10^5 KM12L4a^{Con} or KM12L4a$^{TGF-β}$ cells. Intensities were normalized to day 0 and arbitrarily set to 100. Values are mean ± SEM (*p < 0.05).

(G and H) Inducible TGF-β cells and recipient mice were treated as in Figure 3G. (G) Bioluminescence over time after injection with 5 × 10^5 cells. Values, normalized as in (F), are mean ± SEM (*p < 0.05). (H) Number of liver metastases at time of sacrifice. Whiskers: Vmin, Vmax (*p < 0.05, two-tailed Student's t test).

(I and J) p-SMAD2 staining in liver metastasis generated from KM12L4a^{Con} (I) or KM12L4a$^{TGF-β}$ cells (J). E, epithelial cells; Str, stromal cells. Scale bars = 10 μm.

(K) Relative expression levels of some stromal TBRS genes in dissected metastatic nodules. Values are mean ± SEM (n = 3).

See also Figure S4.

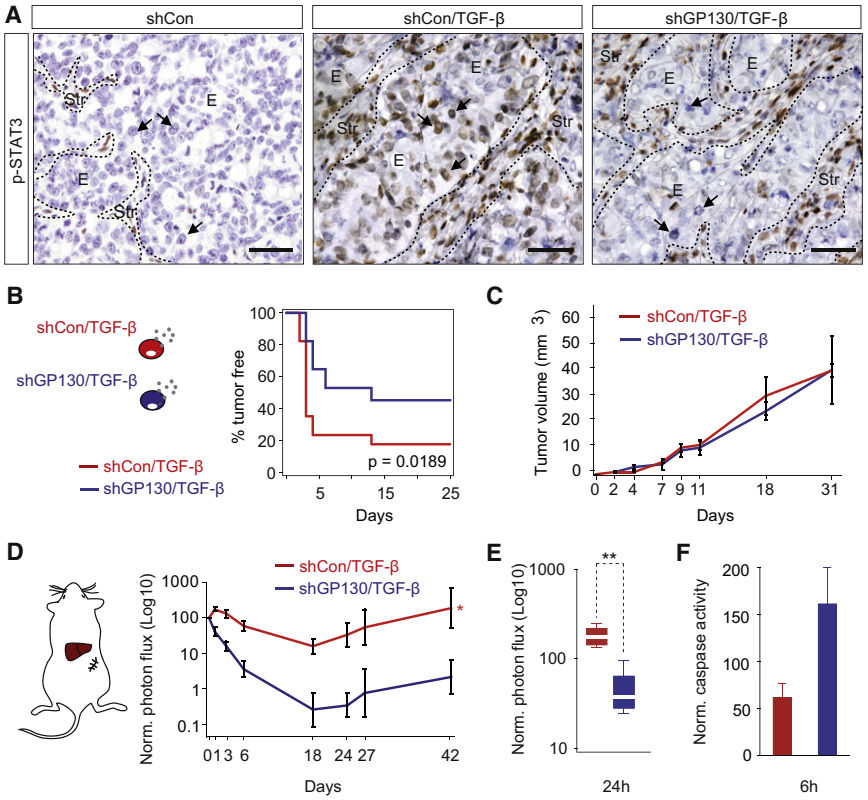

Figure 6. Metastasis Initiation Driven by Stromal TGF-β Signaling Requires GP130/STAT3 in Tumor Cells

(A) p-STAT3 staining in s.c. tumors derived from control (HT29-M6^{shCon}, left panel) cells, HT29-M6 cells that secrete TGF-β (HT29-M6$^{shCon/TGF-β}$, middle panel), or HT29-M6 shGP130 cells that also secrete TGF-β (HT29-M6$^{shGP130/TGF-β}$, right panel). Arrows point to epithelial tumor cell nuclei. E, epithelial cells; Str, stromal cells. Scale bars = 50 μm.

(B) Kaplan-Meier curves for mice injected with 3 × 10^4 HT29-M6$^{shGP130/TGF-β}$ (blue) or HT29-M6$^{shCon/TGF-β}$ cells (red; n = 16).

(C) Growth kinetics of HT29-M6$^{shGP130/TGF-β}$ (blue) and HT29-M6$^{shCon/TGF-β}$ (red) s.c. xenografts (n = 5). Day 1: day of first detection. Values are mean ± SEM.

(D) Bioluminescence over time after IS inoculation of 2 × 10^6 HT29-M6$^{shCon/TGF-β}$ (red) or HT29-M6$^{shGP130/TGF-β}$ (blue) cells. Values, normalized as in Figure 4F, are mean ± SEM (n = 4; *p < 0.05).

(E) Bioluminescence from (D) 24 hr after IS injection. Whiskers: Vmin, Vmax (**p < 0.01, two-tailed Student's t test).

(F) In vivo measurement of caspase 3/7 activity in CRC cells 6 hr after IS injection. Values are mean ratios between caspase activity and total cellular bioluminescence ± SEM (n = 3).

See also Figure S5.

(Figure 6D). The initial clearance of tumor cells is concurrent with apoptosis, as shown by measurement of in vivo caspase activity few hours after inoculation (Figure 6F). In the absence of GP130/STAT3 signaling, apoptosis levels were increased, suggesting that this pathway promotes survival in the context of liver colonization.

Interleukin-11, a TGF-β Target Gene in CAFs, Enhances Metastasis Initiation

Interleukin-11 (IL11), a GP130-binding cytokine, was among the genes highly upregulated by TGF-β in colon fibroblast cultures (F-TBRS, Table S4), although microarray measurements of *IL11* mRNA levels did not associate with cancer recurrence in the cohort of patients with CRC (Table S4). HT29-M6 CRC cells responded to recombinant IL11 by activating the GP130/STAT-3 pathway (Figure 7A). Genes upregulated by IL11 in this cell line constituted an IL11-response signature (IL11RS, Table S4). We found that IL11RS expression correlates tightly with both *TGFB* and FTBRS levels in CRC samples (Figure 7B) and predicts disease relapse (Figures 7C and 7D). Purification of stromal populations from primary human CRC samples showed that CAFs were the only source of IL11 in tumors (Figure 7E). Experimental metastasis generated from TGF-β secreting KM12L4a cells showed a marked upregulation of *IL11* (Figure 7F). Importantly, *IL11* mRNA was reduced to control levels upon LY2157299 treatment of mice bearing CRC stem cell-derived tumors (Figure 7F).

We tested the contribution of IL11 to metastasis by engineering CRC cells to autonomously produce this cytokine. Upon implantation in the cecum of mice, we observed no significant differences in the size (not shown), degree of invasion (Figure 7G), or histological appearance of primary tumors developed by control or study groups (Figures S6A–S6C). Yet, KM12L4a^{IL11} cells effectively colonized liver, lungs, distant lymph nodes, and brain, whereas control cells displayed limited metastatic capacity (Figure 7G, inset table). In the same set of experiments, KM12L4a cells expressing IL6, a cytokine closely related to IL11, displayed a marginal increase in metastatic capacity (Figures S6D and S6E). Intrasplenic inoculation of HT29-M6^{IL11} tumor cells confirmed that IL11 enhanced the liver metastatic potential of CRC cells (Figures 7H–7K). The initial kinetics of metastasis upon intrasplenic inoculation demonstrated that IL11-expressing cells were more proficient at colonizing livers than were control cells (Figures 7I and 7J), an effect that was evident as early as 24 hr after inoculation (Figure 7K). IL11 rescued apoptosis of tumor cells during the first hours of liver colonization (Figure 7L). This behavior paralleled that induced by stromal TGF-β through GP130 signaling in CRC cells shown in Figures 6D–6F.

DISCUSSION

Metastasis involves the regeneration of a full-blown tumor from few disseminated cancer cells. This process is intrinsically inefficient, mainly because of the inability of isolated tumor cells to colonize host tissues and reinitiate tumor growth in a different environment (Luzzi et al., 1998; Valastyan and Weinberg, 2011). The most accepted view is that competences to overcome this initial bottleneck result from Darwinian selection of appropriate genetic alterations in CRC cells. It is not clear, however, how

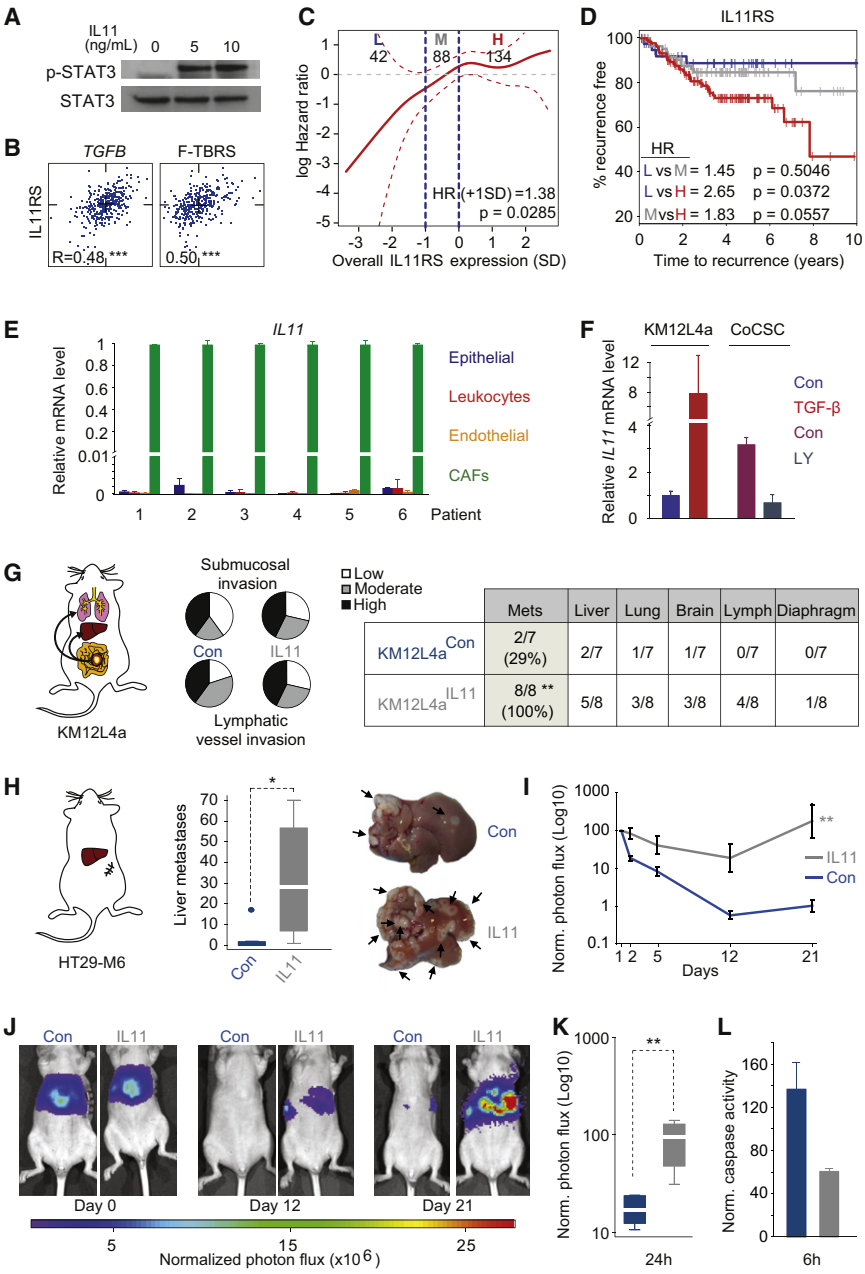

	Mets	Liver	Lung	Brain	Lymph	Diaphragm
KM12L4a^{Con}	2/7 (29%)	2/7	1/7	1/7	0/7	0/7
KM12L4a^{IL11}	8/8 ** (100%)	5/8	3/8	3/8	4/8	1/8

Figure 7. Stromal TGF-β-Induced *IL11* Increases Metastasis Initiation by CRC Cells

(A) Western blot of p-STAT3 and total STAT3 in CRC epithelial cells upon addition of rhIL11.

(B) Cross-correlation analysis between expression of IL11 response signature (IL11RS) and *TGFB* or F-TBRS in the cohort of patients with CRC. Blue dots, patients. R values are indicated (***p < 0.001).

(C) Smooth function correlates IL11RS expression with relative risk of recurrence, patients with stage IV disease excluded. Red dashed lines: 95% CI. Blue dashed lines: thresholds for selection into groups with low (L; blue, 42 patients), medium (M; gray, 88 patients), and high (H; red, 134 patients) IL11RS expression levels. HR (+1SD) and p values are indicated.

(D) Kaplan-Meier plots with RFS for groups defined in (C).

(E) *IL11* mRNA levels in the indicated tumor cell populations from six patients. qRT-PCR values are mean ± SD.

(F) Relative expression levels of *IL11* mRNA in liver metastasis from IS injection with KM12L4a^{Con} (blue) or KM12L4a$^{TGF-β}$ (red) (n = 3) and from s.c. tumors generated by CoCSCs treated with either vehicle (Con, purple) or LY2157299 (dark blue) (n = 2). Values are mean ± SEM.

(G) Pie charts evaluate submucosal or lymphatic vessel invasion in KM12L4a^{con}-derived (n = 7) and KM12L4a^{IL11}-derived (n = 8) cecum tumors. Table shows incidence of metastasis in mice (**p < 0.01, Fisher's exact test).

(H–L) Mice inoculated IS with 2 × 10^6 HT29-M6^{Con} cells (blue; n = 7) or HT29-M6^{IL11} cells (gray; n = 4).

(H) Quantification and representative pictures of liver metastases (arrows) at time of sacrifice (*p < 0.05, two-tailed Student's t test). Whiskers: Vmin, Vmax, truncated at 1.5 times the interquartile range. (I) Bioluminescence over time after IS inoculation. Values, normalized as in Figure 4F, are mean ± SEM (**p < 0.01). (J) Representative images from (I). (K) Bioluminescence 24 hr after injection in mice from (I). Whiskers: Vmin, Vmax (**p < 0.01, two-tailed Student's t test). (L) In vivo caspase 3/7 activity 6 hr after IS injection of HT29-M6^{con} or HT29-M6^{IL11} cells. Values are mean ± SEM.

See also Figure S6.

functions required for colonizing a foreign organ could be selected in the primary tumor where the specific constraints imposed by a different tissue environment are not present (Luzzi et al., 1998; Valastyan and Weinberg, 2011). Additionally, metastatic traits could be acquired after cancer cells have reached the metastatic site, yet this event would necessarily require that tumor cells gain extravasation capacity and survive in the host environment. Our data argue that key functions required to overcome the initial phase of metastasis are provided by the TGF-β-activated microenvironment. Without the activity of this stromal program, fully aggressive CRC cells fail to colonize the host organ. We speculate that those tumor cells capable of initiating metastasis with high efficiency would possess the capacity to raise such TGF-β response in the environment. During metastatic colonization, tumor cells may instruct the stroma of the host organ by either secreting TGF-β or recruiting TGF-β-producing cells such macrophages, CAFs, or platelets. An alternative hypothesis is that a TGF-β-driven premetastatic niche could be specified by the primary tumor in foreign tissues through secretion of systemic cytokines, including TGF-β itself.

Among the benefits that CRCs obtain via crosstalk with the TGF-β-subverted microenvironment is GP130/STAT3 signaling, which suppresses apoptotic stimuli encountered during the colonization of the metastatic site. Fitting these observations, it has been shown that p-STAT3 accumulation in primary CRC samples associates to advanced disease and poor outcome (Kusaba et al., 2006; Morikawa et al., 2011). Indeed, the GP130-binding cytokine IL11, which is secreted by TGF-β

stimulated CAFs, confers robust metastatic capacity to CRC cells. On a side note, IL11 is also a megakaryopoietic cytokine that stimulates platelet production (Musashi et al., 1991; Teramura et al., 1992), and recombinant IL11 is an efficient supportive therapy in patients with malignancies who develop thrombocytopenia as a side effect of chemotherapeutic treatment (Bhatia et al., 2007). Therefore, the prometastatic effect of IL11 described here calls for a reassessment of the use of this cytokine in an adjuvant setting. On the other hand, correlations between elevated platelet counts, referred to as thrombocytosis, and poor prognosis have been reported for many solid cancers, including gastrointestinal tumors (Ikeda et al., 2002; Nouso et al., 2008). Platelets protect circulating tumor cells from immune system, as well as assist them during extravasation (Gay and Felding-Habermann, 2011). In addition, platelets are a rich source of TGF-β (Labelle et al., 2011). It is thus possible that tumor-derived TGF-β may promote IL11 production from stromal cells to increase platelet activation, which may further enhance stromal TGF-β response.

Besides IL11, the TGF-β response signatures include some previously described prometastatic factors in other tumor types, such as ANGPTL4 (Padua et al., 2008), PTHLH (Yin et al., 1999), HBEGF (Bos et al., 2009), CTGF (Kang et al., 2003), TNC (Oskarsson et al., 2011), and JAG1 (Sethi et al., 2011; Sonoshita et al., 2011). For instance, *ANGPTL4* mRNA levels are induced by TGF-β in fibroblasts (Table S4). This secreted factor has been previously shown to mediate intravasation of breast cancer cells into lungs (Padua et al., 2008). Consistent with this observation, our assays show enhancement of lung metastatic capacity by CRC cells upon activation of stromal TGF-β program. JAG1 participates in breast cancer metastasis to the bone (Sethi et al., 2011), and activation of Notch signaling in CRC cells by endothelial cell-expressed JAG1 promotes transendothelial migration during liver and lung metastasis (Sonoshita et al., 2011). Indeed, we found that *JAG1* is a TGF-β response gene in endothelial cells (Table S4). Therefore, besides survival during the colonization phase of metastasis, the program activated by TGF-β in the microenvironment likely influences additional functions required to complete the metastasic process. Importantly, in contrast to CRC, the expression of *ANGPTL4*, *PTHLH*, *CTGF*, or *JAG1* is induced autonomously in breast cancer cells activated by TGF-β (Kang et al., 2003; Padua et al., 2008; Yin et al., 1999). *IL11* itself is a TGF-β target gene in breast cancer cells, with an important role during bone metastasis formation (Kang et al., 2005; Kang et al., 2003). It thus appears that, in the context of a lack of response to TGF-β, CRC cells instead achieve similar abilities by engaging the microenvironment in a TGF-β-dependent manner. It would be interesting to analyze whether this may be a general response in other cancer types that bear inactivating mutations in TGF-β pathway components, such as pancreatic cancer.

The invasive adenocarcinomas developed in mouse models bearing compound mutations in *Smad4* and *Apc* course with a prominent accumulation of reactive stroma (Kitamura et al., 2009; Takaku et al., 1998). Although it is not clear whether this effect depends on increased levels of TGF-β signaling in the microenvironment, *Tgfbr2* deletion in an *Apc* mutant background raises production of TGFB1 in tumors (Muñoz et al., 2006). It is thus plausible that CRCs evolve toward a favorable scenario for metastasis by combining an increase of TGF-β signaling in stromal cells with the acquisition of inactivating mutations in TGF-β pathway components in the cancer cells. The majority of CRCs display moderate-to-high TGF-β expression levels, which may help explain the high rates of CRC metastasis. Importantly, we discovered a subgroup of tumors (10%–20% of all CRCs) displaying invasion and/or local dissemination (i.e., AJCC stage II and III) yet with low TGF-β production that did not relapse after surgical intervention. Therefore, besides AJCC staging, our findings call for the assessment of TGF-β pathway activation in stromal cells as a central criterion for patient stratification. Several targeted therapies against TGF-β signaling, including LY2157299, are currently being evaluated for treatment of different cancer types (Tan et al., 2009; Yingling et al., 2004). Although their efficacy is not yet known, our observations predict that pharmacological inhibition of TGF-β signaling may prevent CRC relapse and metastasis when treating patients at early time point of the process.

EXPERIMENTAL PROCEDURES

Profile Data Sets

We defined overall TGF-β levels (*TGFB*) as the average expression of *TGFB1*, *TGFB2*, and *TGFB3* mRNAs in a given sample (see Supplemental Information). Data sets corresponding to human colon adenomas and carcinomas have been previously described (Sabates-Bellver et al., 2007; Van der Flier et al., 2007). To correlate *TGFB* and TBRS expression with clinical disease progression, we pooled two publicly available sets of Affymetrix transcriptomic profiles (GSE17537 and GSE14333) corresponding to primary CRCs for which clinical follow-up was available. GSE17537 (Smith et al., 2010) is composed of 55 patients with colon cancer treated at Vanderbilt University Medical Center (Nashville, TN, USA). GSE14333 (Jorissen et al., 2009) contains a pool of 290 patients with CRC treated at two different hospitals: Peter MacCallum Cancer Center (Australia) and H. Lee Moffitt Cancer Center (USA). The representation of tumor samples at different AJCC stages in these cohorts follows the natural distribution of patients with CRC receiving standard treatment in the aforementioned hospitals. Descriptive statistics (Table S1) as well as univariate analysis of clinical progression parameters (Table S2) in this metacohort are included as Supplemental Information. The TGF-β response signatures used in this study are detailed in Table S4.

Orthotopic Mouse Studies

All experiments with mouse models were approved by the animal care and use committee of the Barcelona Science Park (CEEA-PCB) and the Catalan Government. Cells were injected subcutaneously in 5–6–week-old Swiss nude or NSG mice (Jackson Laboratories), which were followed for the periods described. Tumor appearance was assessed by palpation. Five-to-six-week-old Balb/c nude or NSG mice (Jackson Laboratories) were used to perform metastasis experiments by intrasplenic injection (Warren et al., 1995) or intracecum injection (Céspedes et al., 2007).

Clinical Material

Biological samples were obtained from individuals treated at the Hospital del Mar (Barcelona, Spain) or from Hospital Clinic (Barcelona, Spain) under informed consent and approval of the Bank Tumor Committees of each hospital according to Spanish Ethical regulations. The study followed the guidelines of the Declaration of Helsinki and patient's identity of pathological specimens remained anonymous in the context of this study. Experiments were approved by the ethics committee of IRB/Hospital Clinic (project ERC-208488/CRCprogramme).

ACCESSION NUMBERS

The transcriptomic data sets generated for this study have been deposited in GEO with accession number GSE39397. This SuperSeries contains the

subset series GSE39394, GSE39395, and GSE39396 as detailed in Supplemental Experimental Procedures.

SUPPLEMENTAL INFORMATION

Supplemental Information includes six figures, four tables, and Supplemental Experimental Procedures and can be found with this article online at http://dx.doi.org/10.1016/j.ccr.2012.08.013.

ACKNOWLEDGMENTS

We thank the Institute for Research in Biomedicine Functional Genomics Core Facility for technical assistance in microarray hybridization experiments, Jonathan Cheng (Fox Chase Cancer Center) for the anti-FAP antibody, Mark Taketo (Kyoto University) for mouse tumor samples, Elisabeth Calderón and Azucena Salas (IDIBAPS, Barcelona) for support with tumor samples, Xavier Hernando for assistance in the animal facility, Jacob Sabates and Giancarlo Marra (IMZR, Zurich) for sharing the Ad-CRC Affymetrix patient data set, Jaume Comas and Ricard Álvarez, (UB, Barcelona) for expert technical assistance with the FACS, Iris Joval for assistance in mounting figures, and all members of the Batlle laboratory for support and discussions. A.C. and D.V.F.T each hold a Juan de la Cierva postdoctoral fellowship, and E.E. has an FPI PhD fellowship (both from Spanish Ministry of Science and Innovation). J.M. is an Investigator of the Howard Hughes Medical Institute. This work has been supported by grants from Instituto de Salud Carlos III FEDER (RD09/0076/00036) and the "Xarxa de Bancs de tumors" sponsored by Pla Director d'Oncologia de Catalunya (XBTC), the European Research Council (Starting Grant no. 208488) and Consolider programmes (MICINN) (both to E.B.), the Spanish Ministry of Science and Innovation (Grants SAF2006-02170 and SAF2009-11757 to E.S.), the National Institutes of Health (Grant CA34610 to J.M.), Fundación BBVA (grant to IRB Barcelona and the Metlab), and Grants PS09/00965 (MICINN) and NanoCoMets (CIBERBBN) (both to R.M.).

Received: February 14, 2012
Revised: June 18, 2012
Accepted: August 17, 2012
Published: November 12, 2012

REFERENCES

Alarcón, C., Zaromytidou, A.I., Xi, Q., Gao, S., Yu, J., Fujisawa, S., Barlas, A., Miller, A.N., Manova-Todorova, K., Macias, M.J., et al. (2009). Nuclear CDKs drive Smad transcriptional activation and turnover in BMP and TGF-beta pathways. Cell *139*, 757–769.

Becker, C., Fantini, M.C., Schramm, C., Lehr, H.A., Wirtz, S., Nikolaev, A., Burg, J., Strand, S., Kiesslich, R., Huber, S., et al. (2004). TGF-beta suppresses tumor progression in colon cancer by inhibition of IL-6 trans-signaling. Immunity *21*, 491–501.

Bhatia, M., Davenport, V., and Cairo, M.S. (2007). The role of interleukin-11 to prevent chemotherapy-induced thrombocytopenia in patients with solid tumors, lymphoma, acute myeloid leukemia and bone marrow failure syndromes. Leuk. Lymphoma *48*, 9–15.

Bos, P.D., Zhang, X.H., Nadal, C., Shu, W., Gomis, R.R., Nguyen, D.X., Minn, A.J., van de Vijver, M.J., Gerald, W.L., Foekens, J.A., and Massagué, J. (2009). Genes that mediate breast cancer metastasis to the brain. Nature *459*, 1005–1009.

Bueno, L., de Alwis, D.P., Pitou, C., Yingling, J., Lahn, M., Glatt, S., and Trocóniz, I.F. (2008). Semi-mechanistic modelling of the tumour growth inhibitory effects of LY2157299, a new type I receptor TGF-beta kinase antagonist, in mice. Eur. J. Cancer *44*, 142–150.

Céspedes, M.V., Espina, C., García-Cabezas, M.A., Trias, M., Boluda, A., Gómez del Pulgar, M.T., Sancho, F.J., Nistal, M., Lacal, J.C., and Mangues, R. (2007). Orthotopic microinjection of human colon cancer cells in nude mice induces tumor foci in all clinically relevant metastatic sites. Am. J. Pathol. *170*, 1077–1085.

Flavell, R.A., Sanjabi, S., Wrzesinski, S.H., and Licona-Limón, P. (2010). The polarization of immune cells in the tumour environment by TGFbeta. Nat. Rev. Immunol. *10*, 554–567.

Gay, L.J., and Felding-Habermann, B. (2011). Contribution of platelets to tumour metastasis. Nat. Rev. Cancer *11*, 123–134.

Grady, W.M., and Markowitz, S.D. (2002). Genetic and epigenetic alterations in colon cancer. Annu. Rev. Genomics Hum. Genet. *3*, 101–128.

Hahn, J.N., Falck, V.G., and Jirik, F.R. (2011). Smad4 deficiency in T cells leads to the Th17-associated development of premalignant gastroduodenal lesions in mice. J. Clin. Invest. *121*, 4030–4042.

Ikeda, M., Furukawa, H., Imamura, H., Shimizu, J., Ishida, H., Masutani, S., Tatsuta, M., and Satomi, T. (2002). Poor prognosis associated with thrombocytosis in patients with gastric cancer. Ann. Surg. Oncol. *9*, 287–291.

Jones, S., Chen, W.D., Parmigiani, G., Diehl, F., Beerenwinkel, N., Antal, T., Traulsen, A., Nowak, M.A., Siegel, C., Velculescu, V.E., et al. (2008). Comparative lesion sequencing provides insights into tumor evolution. Proc. Natl. Acad. Sci. USA *105*, 4283–4288.

Jorissen, R.N., Gibbs, P., Christie, M., Prakash, S., Lipton, L., Desai, J., Kerr, D., Aaltonen, L.A., Arango, D., Kruhøffer, M., et al. (2009). Metastasis-associated gene expression changes predict poor outcomes in patients with Dukes stage B and C colorectal cancer. Clin. Cancer Res. *15*, 7642–7651.

Jung, P., Sato, T., Merlos-Suárez, A., Barriga, F.M., Iglesias, M., Rossell, D., Auer, H., Gallardo, M., Blasco, M.A., Sancho, E., et al. (2011). Isolation and in vitro expansion of human colonic stem cells. Nat. Med. *17*, 1225–1227.

Kang, Y., Siegel, P.M., Shu, W., Drobnjak, M., Kakonen, S.M., Cordón-Cardo, C., Guise, T.A., and Massagué, J. (2003). A multigenic program mediating breast cancer metastasis to bone. Cancer Cell *3*, 537–549.

Kang, Y., He, W., Tulley, S., Gupta, G.P., Serganova, I., Chen, C.R., Manova-Todorova, K., Blasberg, R., Gerald, W.L., and Massagué, J. (2005). Breast cancer bone metastasis mediated by the Smad tumor suppressor pathway. Proc. Natl. Acad. Sci. USA *102*, 13909–13914.

Kim, B.G., Li, C., Qiao, W., Mamura, M., Kasprzak, B., Anver, M., Wolfraim, L., Hong, S., Mushinski, E., Potter, M., et al. (2006). Smad4 signalling in T cells is required for suppression of gastrointestinal cancer. Nature *441*, 1015–1019.

Kitamura, T., Biyajima, K., Aoki, M., Oshima, M., and Taketo, M.M. (2009). Matrix metalloproteinase 7 is required for tumor formation, but dispensable for invasion and fibrosis in SMAD4-deficient intestinal adenocarcinomas. Lab. Invest. *89*, 98–105.

Kusaba, T., Nakayama, T., Yamazumi, K., Yakata, Y., Yoshizaki, A., Inoue, K., Nagayasu, T., and Sekine, I. (2006). Activation of STAT3 is a marker of poor prognosis in human colorectal cancer. Oncol. Rep. *15*, 1445–1451.

Labelle, M., Begum, S., and Hynes, R.O. (2011). Direct signaling between platelets and cancer cells induces an epithelial-mesenchymal-like transition and promotes metastasis. Cancer Cell *20*, 576–590.

Liu, F., Pouponnot, C., and Massagué, J. (1997). Dual role of the Smad4/DPC4 tumor suppressor in TGFbeta-inducible transcriptional complexes. Genes Dev. *11*, 3157–3167.

Luzzi, K.J., MacDonald, I.C., Schmidt, E.E., Kerkvliet, N., Morris, V.L., Chambers, A.F., and Groom, A.C. (1998). Multistep nature of metastatic inefficiency: dormancy of solitary cells after successful extravasation and limited survival of early micrometastases. Am. J. Pathol. *153*, 865–873.

Markowitz, S.D., and Bertagnolli, M.M. (2009). Molecular origins of cancer: molecular basis of colorectal cancer. N. Engl. J. Med. *361*, 2449–2460.

Markowitz, S., Wang, J., Myeroff, L., Parsons, R., Sun, L., Lutterbaugh, J., Fan, R.S., Zborowska, E., Kinzler, K.W., Vogelstein, B., et al. (1995). Inactivation of the type II TGF-beta receptor in colon cancer cells with microsatellite instability. Science *268*, 1336–1338.

Massagué, J. (2008). TGFbeta in Cancer. Cell *134*, 215–230.

Merlos-Suárez, A., Barriga, F.M., Jung, P., Iglesias, M., Céspedes, M.V., Rossell, D., Sevillano, M., Hernando-Momblona, X., da Silva-Diz, V., Muñoz, P., et al. (2011). The intestinal stem cell signature identifies colorectal cancer stem cells and predicts disease relapse. Cell Stem Cell *8*, 511–524.

Morikawa, K., Walker, S.M., Nakajima, M., Pathak, S., Jessup, J.M., and Fidler, I.J. (1988). Influence of organ environment on the growth, selection,

and metastasis of human colon carcinoma cells in nude mice. Cancer Res. *48*, 6863–6871.

Morikawa, T., Baba, Y., Yamauchi, M., Kuchiba, A., Nosho, K., Shima, K., Tanaka, N., Huttenhower, C., Frank, D.A., Fuchs, C.S., and Ogino, S. (2011). STAT3 expression, molecular features, inflammation patterns, and prognosis in a database of 724 colorectal cancers. Clin. Cancer Res. *17*, 1452–1462.

Muñoz, N.M., Upton, M., Rojas, A., Washington, M.K., Lin, L., Chytil, A., Sozmen, E.G., Madison, B.B., Pozzi, A., Moon, R.T., et al. (2006). Transforming growth factor beta receptor type II inactivation induces the malignant transformation of intestinal neoplasms initiated by Apc mutation. Cancer Res. *66*, 9837–9844.

Musashi, M., Yang, Y.C., Paul, S.R., Clark, S.C., Sudo, T., and Ogawa, M. (1991). Direct and synergistic effects of interleukin 11 on murine hemopoiesis in culture. Proc. Natl. Acad. Sci. USA *88*, 765–769.

Nouso, K., Ito, Y., Kuwaki, K., Kobayashi, Y., Nakamura, S., Ohashi, Y., and Yamamoto, K. (2008). Prognostic factors and treatment effects for hepatocellular carcinoma in Child C cirrhosis. Br. J. Cancer *98*, 1161–1165.

Oskarsson, T., Acharyya, S., Zhang, X.H., Vanharanta, S., Tavazoie, S.F., Morris, P.G., Downey, R.J., Manova-Todorova, K., Brogi, E., and Massagué, J. (2011). Breast cancer cells produce tenascin C as a metastatic niche component to colonize the lungs. Nat. Med. *17*, 867–874.

Padua, D., Zhang, X.H., Wang, Q., Nadal, C., Gerald, W.L., Gomis, R.R., and Massagué, J. (2008). TGFbeta primes breast tumors for lung metastasis seeding through angiopoietin-like 4. Cell *133*, 66–77.

Sabates-Bellver, J., Van der Flier, L.G., de Palo, M., Cattaneo, E., Maake, C., Rehrauer, H., Laczko, E., Kurowski, M.A., Bujnicki, J.M., Menigatti, M., et al. (2007). Transcriptome profile of human colorectal adenomas. Mol. Cancer Res. *5*, 1263–1275.

Sato, T., Stange, D.E., Ferrante, M., Vries, R.G., Van Es, J.H., Van den Brink, S., Van Houdt, W.J., Pronk, A., Van Gorp, J., Siersema, P.D., and Clevers, H. (2011). Long-term expansion of epithelial organoids from human colon, adenoma, adenocarcinoma, and Barrett's epithelium. Gastroenterology *141*, 1762–1772.

Sethi, N., Dai, X., Winter, C.G., and Kang, Y. (2011). Tumor-derived JAGGED1 promotes osteolytic bone metastasis of breast cancer by engaging notch signaling in bone cells. Cancer Cell *19*, 192–205.

Shultz, L.D., Ishikawa, F., and Greiner, D.L. (2007). Humanized mice in translational biomedical research. Nat. Rev. Immunol. *7*, 118–130.

Smith, J.J., Deane, N.G., Wu, F., Merchant, N.B., Zhang, B., Jiang, A., Lu, P., Johnson, J.C., Schmidt, C., Bailey, C.E., et al. (2010). Experimentally derived metastasis gene expression profile predicts recurrence and death in patients with colon cancer. Gastroenterology *138*, 958–968.

Sonoshita, M., Aoki, M., Fuwa, H., Aoki, K., Hosogi, H., Sakai, Y., Hashida, H., Takabayashi, A., Sasaki, M., Robine, S., et al. (2011). Suppression of colon cancer metastasis by Aes through inhibition of Notch signaling. Cancer Cell *19*, 125–137.

Subramanian, A., Tamayo, P., Mootha, V.K., Mukherjee, S., Ebert, B.L., Gillette, M.A., Paulovich, A., Pomeroy, S.L., Golub, T.R., Lander, E.S., and Mesirov, J.P. (2005). Gene set enrichment analysis: a knowledge-based approach for interpreting genome-wide expression profiles. Proc. Natl. Acad. Sci. USA *102*, 15545–15550.

Takaku, K., Oshima, M., Miyoshi, H., Matsui, M., Seldin, M.F., and Taketo, M.M. (1998). Intestinal tumorigenesis in compound mutant mice of both Dpc4 (Smad4) and Apc genes. Cell *92*, 645–656.

Tan, A.R., Alexe, G., and Reiss, M. (2009). Transforming growth factor-beta signaling: emerging stem cell target in metastatic breast cancer? Breast Cancer Res. Treat. *115*, 453–495.

Teramura, M., Kobayashi, S., Hoshino, S., Oshimi, K., and Mizoguchi, H. (1992). Interleukin-11 enhances human megakaryocytopoiesis in vitro. Blood *79*, 327–331.

Tsushima, H., Ito, N., Tamura, S., Matsuda, Y., Inada, M., Yabuuchi, I., Imai, Y., Nagashima, R., Misawa, H., Takeda, H., et al. (2001). Circulating transforming growth factor beta 1 as a predictor of liver metastasis after resection in colorectal cancer. Clin. Cancer Res. *7*, 1258–1262.

Valastyan, S., and Weinberg, R.A. (2011). Tumor metastasis: molecular insights and evolving paradigms. Cell *147*, 275–292.

Van der Flier, L.G., Sabates-Bellver, J., Oving, I., Haegebarth, A., De Palo, M., Anti, M., Van Gijn, M.E., Suijkerbuijk, S., Van de Wetering, M., Marra, G., and Clevers, H. (2007). The intestinal Wnt/TCF signature. Gastroenterology *132*, 628–632.

Walther, A., Johnstone, E., Swanton, C., Midgley, R., Tomlinson, I., and Kerr, D. (2009). Genetic prognostic and predictive markers in colorectal cancer. Nat. Rev. Cancer *9*, 489–499.

Wang, J., Sun, L., Myeroff, L., Wang, X., Gentry, L.E., Yang, J., Liang, J., Zborowska, E., Markowitz, S., Willson, J.K., et al. (1995). Demonstration that mutation of the type II transforming growth factor beta receptor inactivates its tumor suppressor activity in replication error-positive colon carcinoma cells. J. Biol. Chem. *270*, 22044–22049.

Warren, R.S., Yuan, H., Matli, M.R., Gillett, N.A., and Ferrara, N. (1995). Regulation by vascular endothelial growth factor of human colon cancer tumorigenesis in a mouse model of experimental liver metastasis. J. Clin. Invest. *95*, 1789–1797.

Yin, J.J., Selander, K., Chirgwin, J.M., Dallas, M., Grubbs, B.G., Wieser, R., Massagué, J., Mundy, G.R., and Guise, T.A. (1999). TGF-beta signaling blockade inhibits PTHrP secretion by breast cancer cells and bone metastases development. J. Clin. Invest. *103*, 197–206.

Yingling, J.M., Blanchard, K.L., and Sawyer, J.S. (2004). Development of TGF-beta signalling inhibitors for cancer therapy. Nat. Rev. Drug Discov. *3*, 1011–1022.